Available online at www.sciencedirect.com

SciVerse ScienceDirect

Ceramics International 39 (2013) 941–946

CERAMICS INTERNATIONAL

www.elsevier.com/locate/ceramint

Thermoelectric properties of Yb-doped $La_{0.1}Sr_{0.9}TiO_3$ ceramics at high temperature

Hongchao Wang[a,*], Chunlei Wang[b]

[a]School of mechanical Engineering, Yonsei University, Seoul, Republic of Korea
[b]School of Physics, State Key Laboratory of Crystal Materials, Shandong University, Jinan, PR China

Received 10 June 2012; received in revised form 1 July 2012; accepted 2 July 2012
Available online 10 July 2012

Abstract

The effect of ytterbium doping on the thermoelectric properties of $La_{0.1}Sr_{0.9}TiO_3$ ceramics has been investigated at the temperature range between 300 K and 1000 K. Samples with different ytterbium concentrations have been synthesized by the conventional solid state reaction technique. An X-ray diffraction pattern suggests that the dominant crystal structure is of perovskite, with a small amount of pyrochlore phase of $Yb_2Ti_2O_7$. The electrical resistivities of all samples exhibit a minimum in the temperature range between 300 K and 1000 K. The minimum values of electrical resistivity are 1.5 mΩ cm, 2.0 mΩ cm, 3.9 mΩ cm, 7.1 mΩ cm, and 9.0 mΩ cm for $x=0.01$, 0.03, 0.05, 0.07, and 0.10, respectively. With the increasing ytterbium content, the electrical resistivity enhanced dramatically, the Seebeck coefficients are increased marginally, and the thermal conductivities are reduced moderately. The lowest thermal conductivity of 3.9 W/mK is obtained in sample of $La_{0.1}Sr_{0.89}Yb_{0.01}TiO_3$, which exhibits maximum figure of merit 0.20 at 963 K.

Keywords: D. Transition metal oxides; C. Electrical properties; C. Thermal conductivity

1. Introduction

The performance of thermoelectric materials is usually evaluated in terms of the thermoelectric figure of merit ZT defined by

$$ZT = S^2T/\rho\kappa \quad (1)$$

where S is the Seebeck coefficient, ρ is the electrical resistivity, κ is the thermal conductivity, and T is the absolute temperature. Therefore, good thermoelectric performance requires a high power factor (PF) $S^2\sigma$, and a low thermal conductivity κ.

Since good thermoelectric performance has been found in $NaCo_2O_4$ single crystals by Terasaki et al. [1], oxide thermoelectric materials have attracted much attention as promising p-type materials for thermoelectric power generators in the high temperature region. Many kinds of Co-based oxides such as $Ca_3Co_4O_9$ [2,3] and Bi–Ca–Co–O [4] have been studied to search for high thermoelectric performance. For a counter-part component, n-type oxide thermoelectric materials with matched thermoelectric properties are required. Up to now, several n-type oxide materials such as $SrTiO_3$ [5–11], $CaMnO_3$ [12] and ZnO [13] et al. have been reported with good thermoelectric properties. Doped $SrTiO_3$ as potential candidate for n-type oxide thermoelectric material has attracted much attention. Okuda et al. [5] have reported that lanthanum-doped $SrTiO_3$ single crystal exhibits high power factor, and its thermoelectric property could be comparable with that of Bi–Te alloy at room temperature. However, its high thermal conductivity reduces its thermoelectric performance, a figure of merit of 0.15 has been obtained for $Sr_{0.95}La_{0.05}TiO_3$ single crystal at 773 K. A figure of merit of 0.21 has been obtained for (La,Sr)TiO_3 ceramics [7]. The enhancement of the figure of merit is mainly due to the reduction of the thermal conductivity by the grain boundaries. Ohta et al. [8–9] has fabricated niobium-doped $SrTiO_3$ epitaxial films, polycrystals, and single crystal with figure of merit values reaching 0.37 at 1000 K, 0.35 at 1000 K, and 0.17 at 1073 K, respectively. In order to increase the figure of merit by reducing the thermal conductivity, we have studied the thermoelectric properties of dysprosium-doped $La_{0.1}Sr_{0.9}TiO_3$

*Corresponding author. Tel.: +82 2 2123 7849; fax: +82 2 312 2159.
E-mail address: wanghongchao@yonsei.ac.kr (H. Wang).

0272-8842/$36.00
http://dx.doi.org/10.1016/j.ceramint.2012.07.009

ceramics [11]. A relatively low thermal conductivity of 2.5 W/m K has been achieved. , Figure of merit for $La_{0.1}Sr_{0.83}Dy_{0.07}TiO_3$ has reached 0.36 at 1045 K, which was the largest value ever reported among $SrTiO_3$ thermoelectric ceramics. The lattice thermal conductivity is associated with the ion mass difference between dopant and matrix [14]. The mass difference between ytterbium and strontium is larger than that of between dysprosium and strontium. In this sense, ytterbium doped $La_{0.1}Sr_{0.9}TiO_3$ ceramics may reduce the lattice thermal conductivity in comparison with dysprosium doped samples. Therefore, doping ytterbium would decrease the thermal conductivity, and improve the figure of merit. From this point, ytterbium doped $La_{0.1}Sr_{0.9}TiO_3$ ceramic samples were prepared in this work, and their thermoelectric properties were studied.

2. Experimental

Ceramic samples of $La_{0.1}Sr_{0.9-x}Yb_xTiO_3$ with $x=0.01$, 0.03, 0.05, 0.07, 0.10 were prepared by conventional solid state reaction technique. The starting materials were La_2O_3 with purity of 99.99%, $SrCO_3$ of 99%, TiO_2 of 99.8%, and Yb_2O_3 of 99.99%, respectively, which were supplied by the Sinopharm Chemical Reagent Co.,Ltd. The raw materials were weighted in stoichiometric proportions, and mixed by ball milling using zirconia balls and ethanol as media for 12 h. After the wet mixtures were dried, they were pressed into pellets, and calcined at 1350 °C for 6 h in ambient air. The pellets were smashed and ball-milled for 12 h. Then the powder was repressed into pellets. These pellets were sintered at 1460 °C for 4 h in the presence of argon gas with 5 mol% hydrogen. The sintered disks were cut into rectangular columns ($20 \times 1.8 \times 1.8$ mm^3) for electric property measurements.

Crystal structure was characterized by X-ray powder diffraction with Cu Kα radiation ($\lambda=0.154056$ nm) utilizing a Bruker AXS D8 ADVANCE diffractometer. Surface morphology was investigated on JSM-840 scanning electronic microscope (SEM). The electrical resistivity and the Seebeck coefficient were measured simultaneously in the temperature range of 300–1000 K using a ULVAC ZEM-3 equipment in helium atmosphere. The thermal diffusivity (λ) and the specific heat capacity (C_p) were measured with Standard Laser Flash Thermal Constants Analyzer ULVAC TC-7000. The densities (d) were measured by the Archimedes' method. The thermal conductivity values (κ)) were calculated from the thermal diffusivity (λ), the specific heat capacity (C_p), and the density (d) by applying the relationship $\kappa=\lambda C_p d$. The power factor and ZT were calculated from the above-measured parameters.

3. Results and discussion

Fig. 1 shows the XRD patterns of the samples with different ytterbium contents at room temperature. We can see from diffraction peaks that the sample with $x=0.01$ only has dominant peaks of $SrTiO_3$, no other peaks are appeared in

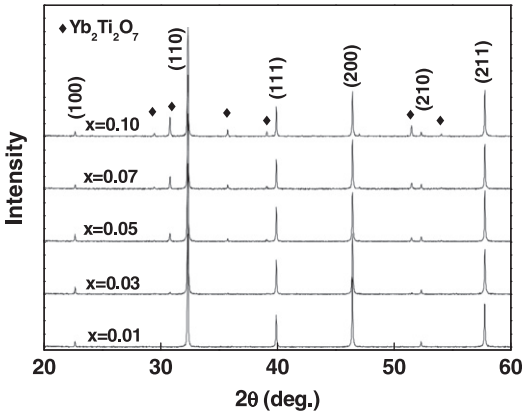

Fig. 1. X-ray powder diffraction patterns of $La_{0.1}Sr_{0.9-x}Yb_xTiO_3$ with $x=0.01$, 0.03, 0.05, 0.07, 0.10 ceramics.

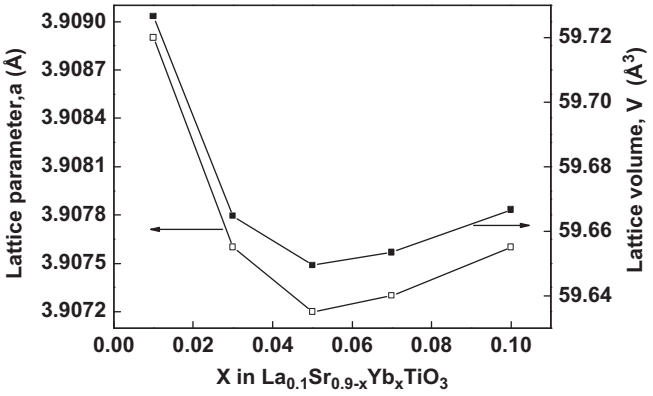

Fig. 2. Lattice constants and cell volumes of $La_{0.1}Sr_{0.9-x}Yb_xTiO_3$ for different x.

XRD pattern. With more ytterbium doped in $La_{0.1}Sr_{0.9}TiO_3$, peaks of secondary phase with pyrochlore structured $Yb_2Ti_2O_7$ have appeared. Moreover, the peak intensity of $Yb_2Ti_2O_7$ increases with the increasing of ytterbium content. These main peaks of all samples have been indexed with the cubic perovskite structure belonging to the Pm3m space group. The lattice constants and cell volumes were calculated from these XRD data. Specifically, they were derived from the indices of crystal face of main peaks and corresponding angles. Because it is difficult to confirm the precise amount of secondary phase, we do not consider the indices of crystal face of secondary peaks and corresponding angles in the calculated progress. The calculated lattice constants and volumes are shown in Fig. 2. The lattice constants and volumes show a non-monotonic relationship with ytterbium contents. Sample with $x=0.05$ posses the smallest lattice constant and volume of 3.8072 Å and 59.6495 Å^3. Deviation from this ytterbium content, the lattice constants and volumes become larger. The sharp decrease of lattice constant and volume from $x=0.01$ to 0.03 is attributed to the smaller ion radius of ytterbium (0.86 Å) than that of strontium (1.12 Å). Variations of lattice constants and volumes for $x=0.03$, 0.05, 0.07, 0.10 are not very obvious, which may be resulted from that the Yb^{3+} can not be fully incorporated into the

$La_{0.1}Sr_{0.9}TiO_3$ lattice when more ytterbium is added. The densities are 4.7024 g/cm^3, 4.6907 g/cm^3, 4.6304 g/cm^3, 4.6064 g/cm^3, 4.8613 g/cm^3 for $x=0.01$, 0.03, 0.05, 0.07, 0.10, respectively. The relative densities are calculated from the measured density over the theoretical density. Because the precise amount of the secondary phase is difficult to determine, theoretical densities are calculated by using the lattice constants from XRD. Therefore, the relative densities are only approximate values. The relative densities are 89%, 88%, 86%, 85.0%, 88% for $x=0.01$, 0.03, 0.05, 0.07, 0.10, respectively.

Fig. 3(a–e) shows scanning electronic microscope (SEM) images of surface microstructures for $La_{0.1}Sr_{0.9-x}Yb_xTiO_3$ ceramics. These images exhibit the typical morphology of sintered ceramics obtained by the solid state reaction. We can easily find from the SEM images that there are fine grains, and the number of fine grains increases with the increasing concentration of ytterbium. We believe that these fine grains are the secondary phase. The sample for $x=0.01$ also has fine grains in the image of SEM; however the XRD pattern shows no secondary phase peaks form Fig. 1. This implies that secondary phase could exist in the $x=0.01$ sample, it is undetectable from XRD. In other words, the $x=0.01$ sample is also not in pure cubic $SrTiO_3$ phase, but the amount of secondary phase is very small. Also we can see from these SEM images that the grain size for main phase decreases with the increase of ytterbium, which indicates that the secondary phase $Yb_2Ti_2O_7$ can inhibit the grain growth for main phase. The appearance of secondary phase might decrease the thermal conductivity.

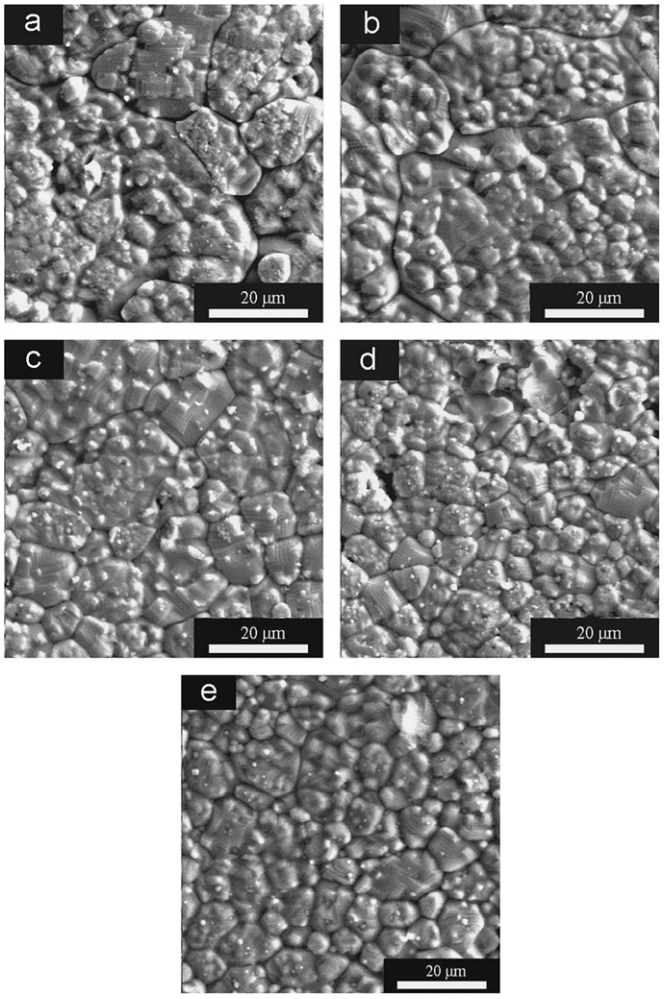

Fig. 3. SEM images of surface section for $La_{0.1}Sr_{0.9-x}Yb_xTiO_3$ ceramics for $x=0.01$, 0.03, 0.05, 0.07, 0.10 as in a, b, c, d, e, respectively.

Temperature dependence of the electrical resistivity is shown in Fig. 4. At low temperatures, the electrical resistivity decrease with the increase in temperature, which is indicative of a semiconductive behavior. This behavior is in accordance with the previous reports in ceramic samples [6,11], but not observed in single crystal samples [5]. This behavior could attribute to the scattering of grain boundaries. With the further increase of temperature, the electrical resistivity of all samples shows a typical metallic behavior. The transition temperature of semiconductive–metallic gradually shifts to high temperatures with increasing of ytterbium content. The electrical resistivity for all samples increases with the increase of ytterbium content. The minimum electrical resistivity has increased from 1.5 mΩ cm for $x=0.01$ to 9.0 mΩ cm for $x=0.10$. Since the electrical resistivity depends on the carrier concentration and carrier mobility, the behavior of the electrical resistivity can be understood from the knowledge of carrier concentration or carrier mobility. With the increase of ytterbium content, the Yb^{3+} can not be fully incorporated into the $La_{0.1}Sr_{0.9}TiO_3$ lattice, and the secondary phase appears accordingly. So we consider that the carrier concentration is not obviously changed. However, in the samples with more amount of secondary phases and hence of finer gain size, more amount of grain boundaries results in reduced carrier mobility. Therefore, the increase of electrical resistivity results from the reducing of carrier mobility.

The temperature dependence of Seebeck coefficient is shown in Fig. 5. The Seebeck coefficients are all negative, indicating n-type conduction mechanism. The Seebeck

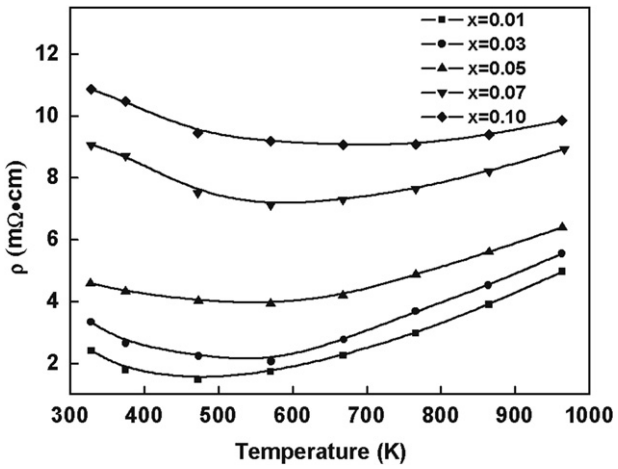

Fig. 4. Temperature dependence of electrical resistivity for $La_{0.1}Sr_{0.9-x}Yb_xTiO_3$ ceramics.

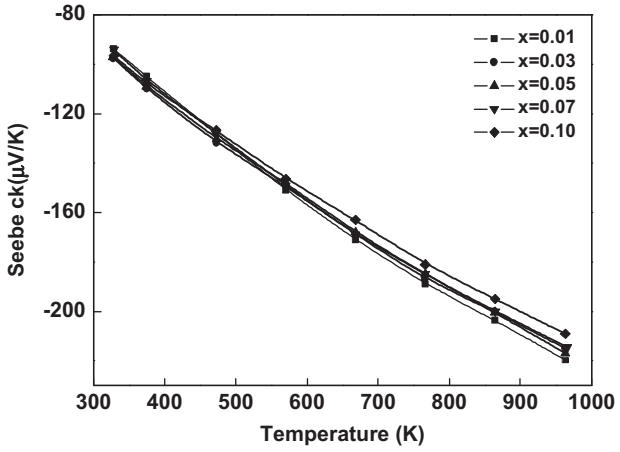

Fig. 5. Temperature dependence of the Seebeck coefficients for $La_{0.1}Sr_{0.9-x}Yb_xTiO_3$ ceramics.

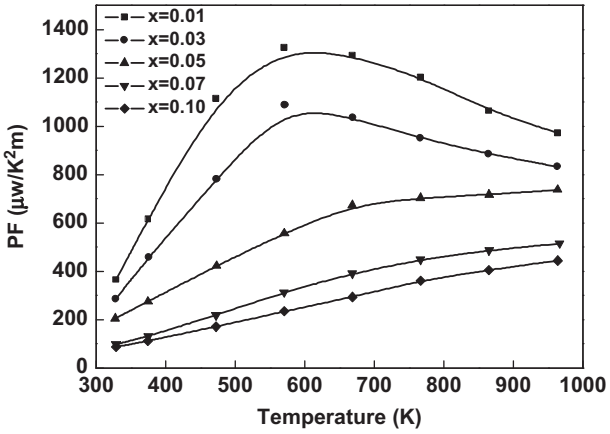

Fig. 6. Temperature dependence of the power factor for $La_{0.1}Sr_{0.9-x}Yb_xTiO_3$ ceramics.

coefficients for all samples change almost linearly with temperature, showing a metallic behavior. This behavior is in agreement with that of degenerate semiconductors in this temperature range [15]. The absolute Seebeck coefficient slightly increased with ytterbium content changing from $x=0.01$ to $x=0.03$. With the further increase of ytterbium content, the Seebeck coefficient is influenced weakly by the ytterbium content. For degenerate semiconductors, in which a parabolic band and energy-independent scattering approximation can be assumed [16], the Seebeck coefficient can be given by the following equation:

$$S = 8\pi^2 K_B{}^2 m^* q T \left(\pi/3n\right)^{2/3}/3eh^2 \quad (2)$$

where K_B, h, m^* and n are Boltzmann constant, Planck constant, the effective mass of the carriers, and carrier concentration, respectively. Eq. (2) indicates that the Seebeck coefficient strongly depends on carrier concentration and effective mass of the carriers. As we can see from Fig. 5 the Seebeck coefficient is not obviously affected by ytterbium contents, this behavior implies that the ytterbium doping does not affect carrier concentration and the effective mass of the carriers. This is also consistent with the previous XRD description that Yb^{3+} cannot be fully incorporated into the $La_{0.1}Sr_{0.9}TiO_3$ lattice when more ytterbium is doped.

Temperature dependence of power factors are calculated from $S^2\sigma$ and presented in Fig. 6 for different ytterbium content. With the increase of temperature, the power factor for $x=0.01$, 0.03 samples displays relative larger values, and has a maximum value of around 600 K. The power factor for samples of $x=0.05$, 0.07, 0.10 increase with increasing of temperature in the whole measured temperature range. The maximum value of power factor for $x=0.01$, 0.03, 0.05, 0.07, 0.10 samples are 1325 $\mu W/K^2m$, 1087 $\mu W/K^2m$, 736 $\mu W/K^2m$, 515 $\mu W/K^2m$, 443 $\mu W/K^2m$, respectively. The temperature corresponding maximum power factor shifts to a higher temperature with more ytterbium doped. We can see that $x=0.01$ ceramic sample exhibits the highest value of power factor, which is mainly attributed to the lower value of electrical resistivity.

Fig. 7 displays the total thermal conductivity (a) and lattice thermal conductivity (b) in temperature range from 300 K to 1000 K. The total thermal conductivity decreases with the increasing of temperature, indicating that the lattice thermal conductivity is dominated. With increase of ytterbium, the total thermal conductivity decreases as we expected. The total thermal conductivity can be expressed by the formula $\kappa=\kappa_L+\kappa_e$, where the κ_L is lattice thermal conductivity and κ_e is the electronic thermal conductivity. The electronic thermal conductivity is calculated from Wiedemann–Franz law as $\kappa_e=LT/\rho$, where Lorentz constant is $L=2.44\times10^{-8}\ V^2K^{-2}$. At high temperature around 973 K, we estimate the electronic contribution to the total thermal conductivity being about 10.3%, 10.0%, 8.9%, 6.6%, 6.1% for $x=0.01$, 0.03, 0.05, 0.07, 0.10, respectively. These values confirm that the total thermal conductivity comes mainly from the lattice vibrations. The lattice thermal conductivity κ_L is estimated from the total thermal conductivity κ and κ_e, and is shown in Fig. 7 (b). The lattice thermal conductivity decreases when ytterbium increases from $x=0.01$ to 0.03, and does not change with further increase of ytterbium. From $x=0.01$ to 0.03, obvious decrease of lattice conductivity is resulted form large difference of ion mass between ytterbium and strontium, this behavior consists with our primary idea. With the further increase of ytterbium content, there is no effect to obvious variation of lattice conductivity, since ytterbium does not fully incorporate into the lattice. Therefore, in low doping level, the reduction of lattice conductivity mainly leads to the decrease of total thermal conductivity. However, at a high doping level, the decrease of total thermal conductivity mainly comes from the reduction of electric thermal conductivity in ytterbium doped $La_{0.1}Sr_{0.9}TiO_3$ ceramics.

Temperature dependence of dimensionless figure of merit ZT is shown in Fig. 8. The ZT value of all samples increases with increasing temperature monotonically over

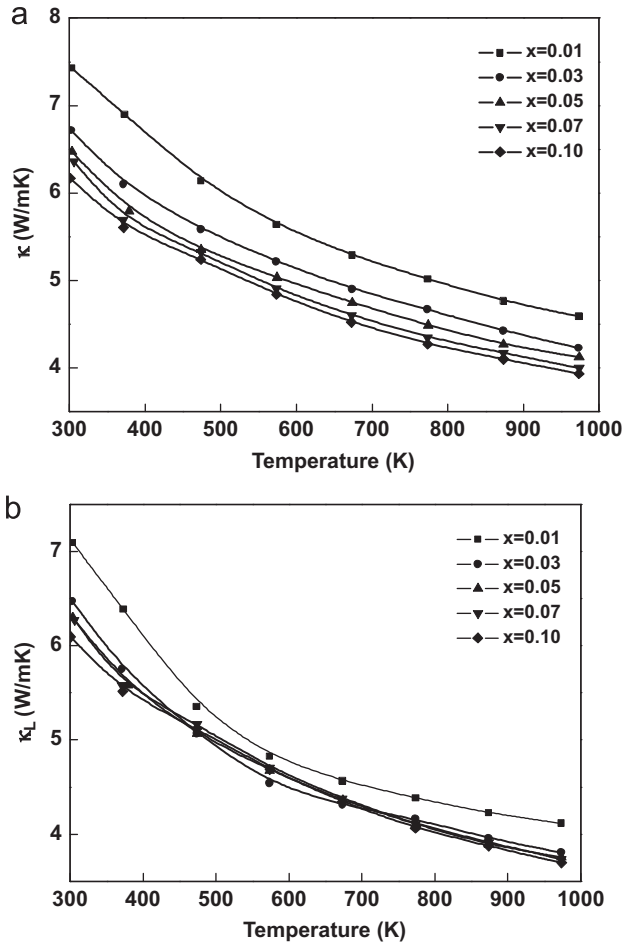

Fig. 7. Temperature dependence of the total thermal conductivity (a) and the lattice thermal conductivity (b) for $La_{0.1}Sr_{0.9-x}Yb_xTiO_3$ ceramics.

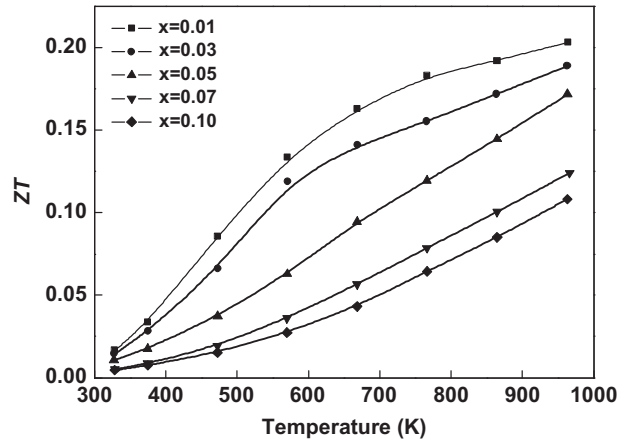

Fig. 8. Temperature dependence of the figure of merit of $La_{0.1}Sr_{0.9-x}Yb_xTiO_3$ ceramics.

the whole temperature range, and decreases with increasing of ytterbium content. The maximum of ZT values for $x=0.01$, 0.03, 0.05, 0.07, 0.10 samples are 0.20, 0.19, 0.17, 0.12, 0.11, respectively. We can easily see that $La_{0.1}Sr_{0.89}Yb_{0.01}TiO_3$ ceramic sample posses the highest ZT value of 0.20 due to its relatively higher power factor. This value is almost same with that of $x=0.00$ sample ($ZT=0.21$) in our previous report [7]. This suggests that the ytterbium doping can reduce the thermal conductivity, and has less effect in enhancing the thermoelectric properties of $La_{0.1}Sr_{0.9}TiO_3$ ceramics.

4. Conclusion

Thermoelectric properties of Yb doped n-type $La_{0.1}Sr_{0.9-}TiO_3$ ceramics are investigated in temperature range between 300 K and 1000 K. All the samples are in cubic perovskite structure with little amount of pyrochlore secondary phase of $Yb_2Ti_2O_7$. Thermal conductivity almost does not changed with doping of ytterbium, electrical resistivity is increased. Also Seebeck coefficient nearly has no influence on the doping of ytterbium. Therefore the figure of merit ZT does not effectively enhance the doping of ytterbium. Our results indicate that doped element ytterbium can improve the electric property, and maintain thermal property and thermoelectric properties of (La, Sr)TiO_3 ceramic nearly remain unchanged.

Acknowledgments

This work is financially supported by the BK 21 HRD program for Nano/Micro Mechanical Engineering, National Basic Research Program of China of 2007CB607504, the Natural Science Fund of China under Grant nos. 50902086 and 50572052, and the Shandong Province Natural Science Foundation under Grant no. ZR2009AQ003. Ms Gaonan Xu is gratefully acknowledged for polishing the English language.

References

[1] I. Terasaki, Y. Sasago, K. Uchinokura, Large thermoelectric power in $NaCo_2O_4$ single crystals, Physical Review B 56 (1997) R12685–R12687.

[2] Y. Liu, Y.H. Lin, Z. Shi, C.W. Nan, Z.J. Shen, Preparation of $Ca_3Co_4O_9$ and improvement of its thermoelectric properties by spark plasma sintering, Journal of the American Ceramic Society 88 (2005) 1337–1340.

[3] H.Q. Liu, X.B. Zhao, T.J. Zhu, Y. Song, F.P. Wang, Thermoelectric properties of Gd, Y co-doped $Ca_3Co_4O_{9-\delta}$, Current Applied Physics 9 (2009) 409–413.

[4] A. Sotelo, E. Guilmeau, Sh. Rasekh, M.A. Madre, S. Marinel, J.C. Diez, Enhancement of the thermoelectric properties of directionally grown Bi–Ca–Co–O through Pb for Bi substitution, Journal of the European Ceramic Society 30 (2010) 1815–1820.

[5] T. Okuda, K. Nakanishi, S. Miyasaka, Y. Tokura, Large thermoelectric response of metallic perovskites: $Sr_{1-x}La_xTiO_3$ ($0 \le x = y \le 0.1$), Physical Review B 63 (2001) 11304.

[6] H.C. Wang, C.L. Wang, W.B. Su, J. Liu, H. Peng, Y. Sun, J.L. Zhang, M.L. Zhao, J.C. Li, N. Yin, L.M. Mei, Synthesis and thermoelectric performance of Ta doped $Sr_{0.9}La_{0.1}TiO_3$ ceramics, Ceram, Intern 37 (2011) 2609–2613.

[7] J. Liu, C.L. Wang, W.B. Su, H.C. Wang, P. Zheng, J.C. Li, J.L. Zhang, L.M. Mei, Enhancement of thermoelectric efficiency in oxygen-deficient $Sr_{1-x}La_xTiO_{3-\delta}$ ceramics, Applied Physics Letters 95 (2009) 162110.

[8] S. Ohta, T. Nomura, H. Ohta, H. Hosono, K. Koumoto, Large thermoelectric performance of heavily Nb-doped $SrTiO_3$ epitaxial film at high temperature, Applied Physics Letters 87 (2005) 092108.
[9] S. Ohta., H. Ohta, K. Koumoto, Grain size dependence of thermoelectric performance of Nb-doped $SrTiO_3$ plyscrystals, Journal of Ceramic Society of Japan 114 (2006) 102–105.
[10] S. Ohta, T. Nomura, H. Ohta, K. Koumoto, High temperature carrier transport and thermoelectric properties of heavily La- or Nb-doped $SrTiO_3$ single crystals, Journal of Applied Physics 97 (2005) 034106.
[11] H.C. Wang, C.L. Wang, W.B. Su, J. Liu, Y. Zhao, H. Peng, J.L. Zhang, M.L. Zhao, J.C. Li, N. Yin, L.M. Mei, Enhancement of thermoelectric figure of merit by doping Dy in $La_{0.1}Sr_{0.9}TiO_3$ ceramic, Materials Research Bulletin 45 (2010) 809–812.
[12] X.Y. Huang, Y. Miyazaki, T. Kajitani, High temperature thermoelectric properties of $Ca_{1-x}Bi_xMn_{1-y}V_yO_{3-\delta}$ ($0 \le x = y \le 0.08$), Solid State Communications 145 (2008) 132–136.
[13] M. Ohtaki, K. Araki, K. Yamamoto, High thermoelectric performance of dually doped ZnO ceramics, Journal of Electronic Materials 38 (2009) 1234–1238.
[14] B. Abeles, Lattice thermal conductivity of disordered semiconductor alloys at high temperatures, Physical Review Letters 131 (1963) 1906–1911.
[15] R. Moos, A. Gnudi, K.H. Hardtl, Thermopower of $Sr_{1-x}La_xTiO_3$ ceramics, Journal of Applied Physics 78 (1995) 5042–5047.
[16] M. Cutler, J.F. Leavy, R.L. Filzpatrick, Electronic transport in semimetallic cerium sulfide, Physical Review Letters 133 (1964) A1143.